Deutschmann, B., Ott, C., Monje, C. A. y Balaguer, C. (2017). Robust Motion Control of a Soft Robotic System Using Fractional Order Control. *In 26th International Conference on Robotics in Alpe-Adria-Danube Region, RAAD 2017: Advances in Service and Industrial Robotics,* Springer, Cham, pp. 147-155.

DOI: https://doi.org/10.1007/978-3-319-61276-8_17

Robust Motion Control of a Soft Robotic System Using Fractional Order Control

Bastian Deutschmann[1], Christian Ott[1] Concepcion A. Monje[2], and Carlos Balaguer[2]

Institute of Robotics and Mechatronics, German Aerospace Center (DLR), Oberpfaffenhofen, 82234, Wessling, Germany,
Bastian.Deutschmann,Christian.Ott@dlr.de.,
1 Systems Engineering and Automation Department, University Carlos III of Madrid, Av. de la Universidad 30, 28911, Leganés, Madrid, Spain

2

Abstract. This work presents a novel control approach for a tendon-driven soft robotic system. The soft robotic system composed of a silicon continuum, tendons and antagonistic actuation yields a highly complex mechanical model. As the high complexity is not feasible here, a linear time invariant system is approximated instead for the controller design. A fractional order PD^{α} controller is applied to meet performance and the high robustness requirements due to the neglected nonlinear dynamics. Simulation and experimental data confirm a superior performance of the FO controller while exhibiting a higher robustness to model missmatches and better disturbance rejection properties.

Keywords: Fractional Order Control, Soft Robotics, Robust Control

1 Introduction

In recent years, inherently soft robots got in focus of research. With this inherent softness, collisions with humans or the environment can be handled by the hardware of the robot [8]. The soft robotic system of the present paper is a prototype for a spine and neck for a future humanoid robot [6] (Fig. 1) and the softness is gained by the use of silicon. The majority of continuum robot systems are steerable catheters [7]. In these systems, the structural flexibility is mainly used to bend continuously whereas axial or shear deformations can be neglected. As these systems are used in positioning tasks with small masses, their control goal is to be accurate in the task space of the system and usually kinematic [1] or kinetic controllers [7] are used. Requirements on performance or robustness have not been investigated since slow motions were of interest. The present system is able to deform considerably in all directions and the higher mass of the system implies higher dynamic effects especially since we are interested in fast motions. To achieve a robust performance of the closed loop system, a FO- controller is designed as it has proven good results for similar requirements and systems in the past [3]. The contribution here will be, that the approach previously published by the authors [4] is extended towards the design of FO lag-compensators and the passivity property of this controller will be investigated, which is, to the authors knowledge the first work in this direction. Furthermore three experiments including the desired nominal behavior, a mass variation and a external

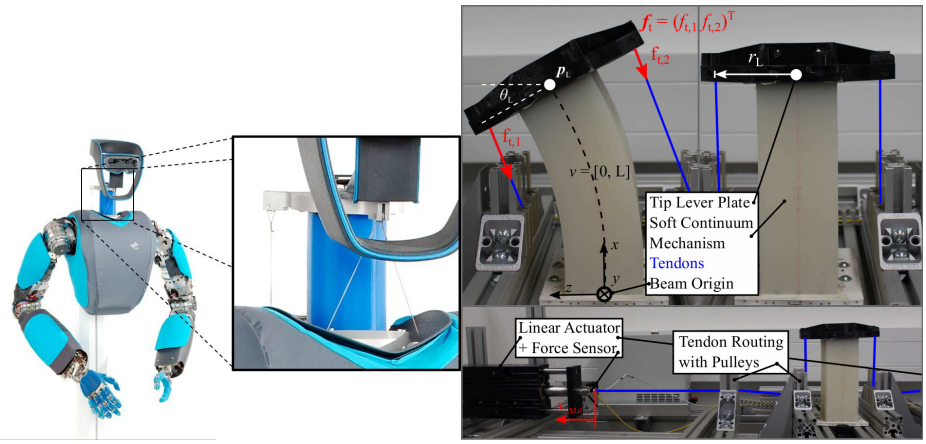

Fig. 1. Left: Tendon-driven soft continuum mechanism as a neck in a humanoid robot [6]. Right: Test setup including two linear actuators which are connected via tendons (blue) to the tip lever plate of the soft continuum mechanism. Top: Close up in straight and deflected configurations. Bottom: Left side of the antagonistic setup.

disturbance experiment underline the good results of the FO controller from simulations in comparison with two standard controllers. The work is structured in five sections. Section 2 presents the control problem and the model equations. The fractional- and integer-order (IO) controllers are designed in 3 and the passivity properties of these controllers are examined. Section 4 reports on all experiments and Section 5 draws the main conclusions of this approach.

2 Problem Statement & System Model

The problem at hand is to control the tip angle $\theta_\mathrm{L} \in \mathbb{R}$ of the planar soft continuum mechanism, see Fig. 1, whereas the control action is the external torque $\tau_\mathrm{L} \in \mathbb{R}$ at the tip generated by two, antagonistically acting tendon forces $\boldsymbol{f}_\mathrm{t} \in \mathbb{R}^2$ of each actuator while measuring tendon forces and tendon positions $\boldsymbol{x}_\mathrm{LM} \in \mathbb{R}^2$ only. As the full dynamic model of this mechanism includes partial differential equations and a nonlinear dynamic coupling between the tip and the actuator motion, it is not suitable for the design of a linear controller. Instead, a linear time invariant transferfunction $G(s) \in \mathbb{R}$ is used as an approximation for the dynamics of $\Theta_\mathrm{L}(s)$ w.r.t. the input $\tau_\mathrm{L}(s)$,

$$G(s) = \frac{K\omega_\mathrm{n}^2}{s^2 + 2\delta\omega_\mathrm{n}s + \omega_\mathrm{n}^2} = \frac{\Theta_\mathrm{L}(s)}{\tau_\mathrm{L}(s)}. \tag{1}$$

with the steady-state gain $K = 0.0631$, the Eigenfrequency of the system $\omega_n = 37.8021$, and the linear damping $\delta = 0.4$. The parameters has been estimated experimentally by measuring step responses. A comparison between the model and the real system can be found in Fig. 2 for the dynamic and the static case.

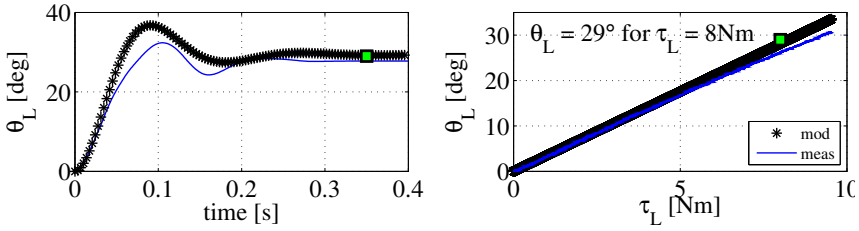

Fig. 2. Comparison of the model (mod) and the real system (meas). Left: Dynamic characteristic with an input step of $\tau_L = 8$Nm. Right: Static characteristic while the mechanism is slowly moved through the workspace.

3 Controller Design

In the following section, three linear controllers will be designed for the system (1): a FO controller, a PID controller and a lag compensator. The controller specification and the constraints are presented subsequently.

3.1 Control Specifications

The controller need to fulfill specifications related to gain crossover frequency ω_{cg}, phase margin φ_{m} due to their important significance regarding performance and stability [5]. The design problem is to find a controller $C(j\omega)$ such that

$$|C(j\omega_{\mathrm{cg}})G(j\omega_{\mathrm{cg}})|_{\mathrm{dB}} = 0\mathrm{dB}, \text{ with } \omega_{\mathrm{cg}} = 3\mathrm{rad/s} \tag{2}$$

$$\arg(C(j\omega_{\mathrm{cg}})G(j\omega_{\mathrm{cg}})) = -\pi + \varphi_{\mathrm{m}}, \text{ with } \varphi_{\mathrm{m}} = 80^\circ \tag{3}$$

$$\left.\frac{d(\arg(C(j\omega)G(j\omega)))}{d\omega}\right|_{\omega=\omega_{\mathrm{cg}}} = 0\mathrm{s} \tag{4}$$

Here, ω_{cg} and φ_{m} were chosen to fulfill a desired performance. The last equation forces the phase of the open loop system to be flat at $\omega = \omega_{\mathrm{cg}}$ and so, to be almost constant within an interval around ω_{cg} yielding more robustness to gain changes and the overshoot of the response is almost constant within a gain range (iso-damping property of the time response).

3.2 FO Controller

As a novel control approach for the soft continuum mechanism, we propose the use of a FO PD^α controller [4] which corresponds to a fractional order lead compensator. The three parameters $\alpha, \lambda, x \in \mathbb{R}$ are obtained with the method in [5]. As the characteristic of our model in combination with the desired φ_{m} demand a phase-lag, the method is extended to the design of a fractional lag compensator. For this case, the controller will be designed as a lead compensator according to [5] giving a phase $|\varphi_{\mathrm{lead}}| = |\varphi_{\mathrm{lag}}|$, and later the sign of α will be changed so that the phase contribution is negative. It has to be taken into account that a change in the sign of α for the lag compensation leads to an inverted magnitude of the designed compensator. To keep the gain unchanged

(fulfilling already the specification of crossover frequency), the lag compensator should be multiplied by a gain $k_{\text{lag}} = 1/\left|G(j\omega_{\text{cg}})\right|^2$ yielding a fractional lag compensator with

$$C_{\text{FOC}}(s) = k_{\text{lag}} \left(\frac{\lambda s + 1}{x\lambda s + 1} \right)^{-\alpha}, \tag{5}$$

Now a FO controller of the form in (5) is designed so that the specifications (2,3,4) are achieved resulting in

$$C_{\text{FOC}}(s) = 905.7688 \left(\frac{6.97s + 1}{0.0069s + 1} \right)^{-1.12}, \tag{6}$$

The Bode plots of the open-loop system with this FO controller are shown in Fig. 3, where it can be observed that the phase margin, gain crossover frequency, and robustness constraints (flat phase) are fulfilled. The implementation of a FO

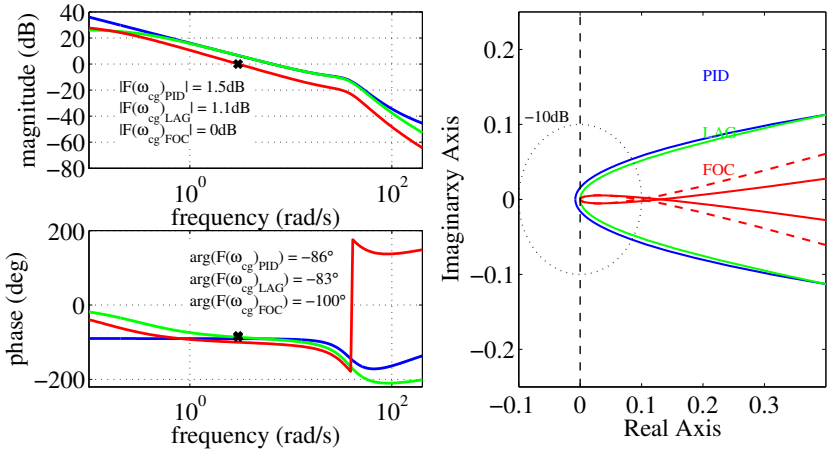

Fig. 3. Left: Bode plots of the open-loop system of all three designed controllers. Right: Nyquist plots of the $P(s)$ functions corresponding to the three controllers. The dashed, red curve corresponds to the finite approximation of the FO controller.

controller is usually done by an IO- approximation. For details and a review see [4]. Here (6) is approximated using the MATLAB© routine *invfreqs* which fits the frequency response of the FO controller in a frequency of two decades around the gain crossover frequency, with two poles/zeros:

$$\tilde{C}_{\text{FOC}}(s) = \frac{0.3908s^2 + 67.3s + 774.4}{s^2 + 7.465s + 0.8204} \tag{7}$$

3.3 IO- controllers

A IO- PID and a IO- LAG compensator are designed with the frequency domain specifications of the previous section. However, as for an IO- controller, the

maximum contribution in phase is $-90°$, therefore (3) can not be met. The PID is tuned with the *Automated PID Tuning* method incorporated in the *Control Systems Toolbox* in MATLAB©. The designed PID controller is

$$C_{\mathrm{PID}}(s) = 41.17 \cdot \frac{(1+0.024s)^2}{s}, \tag{8}$$

whose open-loop Bode plots are presented in Fig. 3 where one can see that (2,3,4) are fulfilled. A physical interpretation of this controller is that by choosing both zeros of (8) to be at $z_{1,2} \approx 41.6$rad/s, the controller approximately cancels the poles of the system (1) and extends the flat phase to the system (see Fig. 3). The general transfer function of an IO- lag compensator incorporates on pole p and one zero z, with $z > p$. Therefore it lacks on parameter and the flat phase robustness constraint (4) cannot be guaranteed. By solving (2) and (3), we find the IO- lag compensator with the Bode plots in Fig. 3 and the transfer function

$$C_{\mathrm{LAG}}(s) = \frac{s+39.74929}{s+0.3007329}. \tag{9}$$

3.4 Passivity Analysis

The controller design in the previous section was based on a linear model. The experimental results in Section 4 will confirm that the inaccuracy in the linear approximation of the system dynamics can be handled by these robustness properties. Subsequently, we want to discuss to which extent one can make analytical stability statements for the application of the (linear) fractional-order controller to the nonlinear system dynamics. In particular, we look at the passivity properties of the closed-loop system. As a purely mechanical structure, the continuum mechanism clearly is a passive system with the physical energy as a storage function, considering the input τ_{L} and the output $\dot{\theta}_{\mathrm{L}}$. This input-output pair represents the physical power between the controller and the mechanism. In the following, we will investigate if the designed controllers represents a passive system w.r.t. the input $\dot{\theta}_{\mathrm{L}}$ and the output $-\tau_{\mathrm{L}}$, i.e. in feedback interconnection with the mechanism. Since passivity is preserved by feedback interconnection of passive subsystems [9], we can then conclude passivity of the closed loop system. For showing the passivity of the controller we have to consider the transfer function $P(s) = -C_{\mathrm{FOC}}(s)\frac{1}{s}$. Passivity requires $\mathrm{Re}(P(j\omega)) \geq 0$ (positive realness) for all frequencies ω, which can be checked with a Nyquist plot. Figure 3, right shows the Nyquist plots of P(s) corresponding the three controllers discussed in the previous sections. One can easily observe that the fractional-order controller as well as its finite-order approximation are positive real, while this is not the case for the PID controller. Notice that this analysis assumes that the electrical dynamics of the force-controlled actuators is sufficiently fast so that it can be neglected and thus the desired control torque τ_{L} can be realized instantaneously. While unmodeled dynamics at the level of the continuum mechanism can be handled in this way, unmodeled dynamics at the actuator level would need a different approach.

4 Experimental Results

The setup used for the experiments is depicted in Fig. 1. Two linear actuators from Linmot© with incorporated position sensors are equipped with an axial

		ISE m^2s			CA 10^4 $(Nm)^2$		
Controller		PID	LAG	FOC	PID	LAG	FOC
Nominal		12.34	17.05	7.63	2.52	2.26	2.94
Mass	1 Mot.	9.56	13.23	5.94	1.88	1.71	2.19
	097	20.91	27.34	13.09	1.87	1.75	2.96
	194	22.07	27.65	12.54	1.82	1.73	2.93
	380	20.51	26.84	12.90	1.82	1.71	2.84
	566	20.72	26.46	12.87	1.73	1.63	2.75
	663	unstable	unstable	12.84	unstable	unstable	2.61
	849	unstable	unstable	12.85	unstable	unstable	2.53
Disturb.	0°	0.90	1.19	0.69	0.28	0.23	0.12
	20°	0.80	0.90	0.40	0.32	0.30	0.25

Table 1. ISE and CA of the three different controllers.

force sensor from Omega© to measure position and external force at each slider. The designed motion controllers are implemented in MATLAB/Simulink© using real time workshop on a QNX-neutrino 6.5 target. An EtherCAT bus sends the generated control signals to the current controller of the linear motors and receives sensor information within a control cycle of 1kHz. The soft continuum mechanism is molded out of silicon from Dragonskin© and connected to a 3D-printed bottom plate and tip plate. The polyethylene tendons are looped around a ball bearing, and are connected to the mechanism at the tip, see Fig. 1. The tendons are routed with pulleys at each side towards the actuators.

4.1 Evaluation

The performance of each controller is evaluated using the ISE- index [2]. The ISE- value is associated to the error energy indicating a small control error, which is desirable. Furthermore, we want to assess the control action by

$$\mathrm{CA} = \frac{1}{t_{\mathrm{end}}} \int_0^{t_{\mathrm{end}}} (\tau_{\mathrm{L}}(t=0) - \tau_{\mathrm{L}}(t))^2 dt \tag{10}$$

to indicate the amount of energy created by the control law. A low CA-value indicates less control action, which is desirable.

4.2 Experiments

Three experiments are present in which all three controllers are examined. 1) A nominal step response with step input of 20°. 2) A nominal step input were additional masses of $m_{\mathrm{ext}} = \{97, 194, 380, 566, 663, 849\}$g are place at the tip of the mechanism to increase the overall inertia and a nominal step were 1 motor is disconnected to reduce the overall inertia. 3) A disturbance test in which a dropdown mass is attached to the tip of the mechanism by a cord to generate reproducible disturbances of the controlled system at the $\theta_{\mathrm{L}} = 0°$ and 20°.

4.3 Results

Fig. 4, left, shows the experimental step responses of the system and respective control laws in closed loop of all controllers. As can be seen in the figure, the FO controller presents a slightly underdamped response (peak value of 20.44°), as expected, and a soft control law below 8Nm. The final value of the response is 19.65°, presenting a small but negligible steady-state error due to the absence of an integral component. The PID presents zero steady-state error due to the effect of the integral action. The lag compensator presents a higher steady-state error (final value of 17.77°). Though the three controlled systems present a transient with similar settling time, the rise time for the FO controller is lower and its steady-state error negligible, providing a better response than the IO- controllers. The assessment of the three controller w.r.t. the performance measures is shown in Table 1. For the nominal response (first line). one can observe that the FO controller has the lowest ISE value, meaning the least error over time to the desired motion. However, the FO controller needs the highest control action, indicated in a higher CA value. In order to test that the device behaves experi-

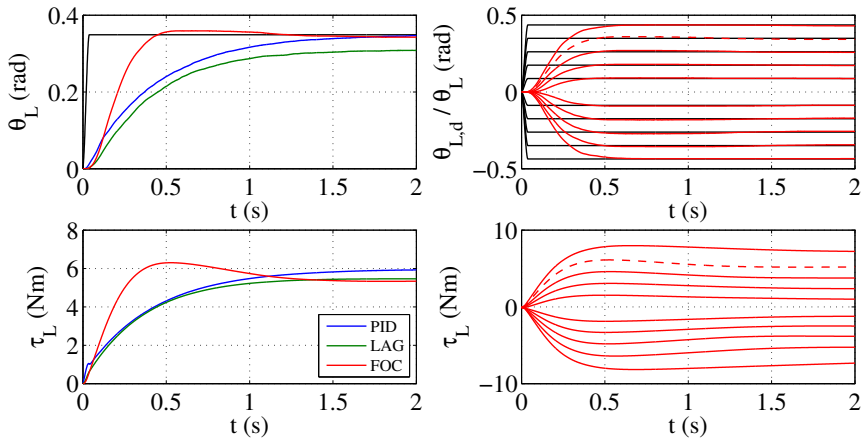

Fig. 4. Left: Experimental step responses θ_{L} of the system in closed-loop and corresponding control inputs τ_{L} of all three controllers. Right: Experimental step responses of the system with the FO controller (red) for different step inputs with amplitudes in the range $(5°, 25°)$.

mentally as a linear system around the nominal working point, the FO control system has been tested for different step inputs with amplitudes in the range $(5°, 25°)$. The results are presented in Fig. 4, right, showing that only slight variations are appreciated w.r.t. the nominal performance. When additional masses are placed at the tip, the FO controller presents a robust performance, while the PID controller and the lag compensator become unstable for $m_{\mathrm{ext}} = 566$g. The reported behaviour is substained by a video that shows the experiments, see https://www.youtube.com/watch?v=ivR-3bN0LVA&feature=youtu.be.
When the closed loop system is disturbed by the drop down mass, a robust performance is obtained in all the cases. However, the disturbance rejection property

of the FO controller is superior to the IO- controllers since the ISE- and the CA-value are both smaller which means that the FO controller needs less power to reject the disturbance, see Tab. 1.

5 Conclusions and Future Works

This paper reports on a model-based approach to control the tip angle of a tendon-driven soft robotic system. The complete nonlinear dynamic model of the system is not feasible here. Therefore, an approximation of a linear time invariant second-order system is used. A FO lag compensator is designed with this model and is proven to be passive. The required specifications for the closed-loop system are met with this controller and the incorporated robustness is able to cope with neglected nonlinear dynamics. In order to compare the FO controller, two standard IO- controllers are designed with the same specifications: a PID controller, which is not passive and a lag compensator, which is passive. All three controllers prove an experimentally stable response. However, FO controller has three major advantages. It exhibits a faster transient response compared to the IO- controllers and at the same time is more robust to unmodelled dynamics and furthermore exhibits a superior disturbance rejection. These three points could be validated within the experiments and two standard measures to assess the controller performance. In the future, we will extend the problem to the multi DoF case to see whether the approach can handle the increased nonlinearity.

References

1. I. A. Gravagne, C. D. Rahn, and I. D. Walker, "Large deflection dynamics and control for planar continuum robots," *IEEE/ASME Transactions on Mechatronics*, vol. 8, no. 2, pp. 299–307, 2003.
2. W. S. Levine, *The control handbook*. CRC press, 1996.
3. C. Monje, F. Ramos, V. Feliu, and B. Vinagre, "Tip position control of a lightweight flexible manipulator using a fractional order controller," *Control Theory & Applications, IET*, vol. 1, no. 5, pp. 1451–1460, 2007.
4. C. A. Monje, Y. Chen, B. M. Vinagre, D. Xue, and V. Feliu-Batlle, *Fractional-order systems and controls: Fundamentals and applications*. Springer Science & Business Media, 2010.
5. C. A. Monje, B. M. Vinagre, V. Feliu, and Y. Chen, "Tuning and auto-tuning of fractional order controllers for industry applications," *Control Engineering Practice*, vol. 16, no. 7, pp. 798–812, 2008.
6. J. Reinecke, B. Deutschmann, and D. Fehrenbach, "A structurally flexible humanoid spine based on a tendon-driven elastic continuum," in *Robotics and Automation (ICRA), 2016 IEEE International Conference on*. IEEE, 2016, pp. 4714–4721.
7. D. C. Rucker and R. J. Webster, "Statics and dynamics of continuum robots with general tendon routing and external loading," *IEEE Transactions on Robotics*, vol. 27, no. 6, pp. 1033–1044, 2011.
8. D. Trivedi, C. D. Rahn, W. M. Kier, and I. D. Walker, "Soft robotics: Biological inspiration, state of the art, and future research," *Applied Bionics and Biomechanics*, vol. 5, no. 3, pp. 99–117, 2008.
9. A. van der Schaft, *L_2-Gain and Passivity Techniques in Nonlinear Control*, 2nd ed. Springer-Verlag, 2000.